

ANALYSIS

View Article Online
View Journal | View IssueCite this: *Energy Environ. Sci.*, 2021, 14, 3686

Comparing pathways for electricity-based production of dimethoxymethane as a sustainable fuel†

Jannik Burre, ^a Dominik Bongartz, ^a Sarah Deutz, ^b Chalachew Mebrahtu, ^c Ole Osterthun, ^c Ruiyan Sun, ^c Simon Völker, ^b André Bardow, ^{bdef} Jürgen Klankermayer, ^c Regina Palkovits ^c and Alexander Mitsos ^{cade}

Synthetic dimethoxymethane (DMM) is a promising fuel or blend component as it offers outstanding combustion characteristics. DMM production from hydrogen (H₂) and carbon dioxide (CO₂) is technically feasible with established technology but results in a low overall process efficiency. Recent research in catalyst development has increased DMM yield significantly and new reaction pathways have been proposed. Yet, it remains unknown how the achievements in catalyst development affect process performance. To close this gap, we analyze processes based on five reaction pathways regarding exergy efficiency, production cost, and climate impact. As the pathways have different technology readiness levels, we develop a methodology that ensures consistent boundary conditions and model detail between pathways. The methodology enables a hierarchical optimization-based process design and evaluation. The results show that the non-oxidative (i.e., reductive, dehydrogenative, and transfer-hydrogenative) pathways consume stoichiometrically less H₂ not only than the established and oxidative pathway, but also less than most other electricity-based fuels (e-fuels). The higher resource efficiency of these pathways increases process exergy efficiency from 75% to 84%; production cost (2.1\$ L_{diesel-eq.}⁻¹) becomes competitive to other e-fuels; and the impact on climate change reduces by up to 92% compared to fossil diesel, if renewable electricity is utilized. Whereas the reductive pathway may already enable a sustainable production of DMM with only little catalyst improvements, the dehydrogenative and transfer-hydrogenative pathways still require a higher DMM selectivity and methanol conversion, respectively. With considerable catalyst improvements, a maximum exergy efficiency of 92% and minimum production cost of 2.0\$ L_{diesel-eq.}⁻¹ are achievable. Our analyses show: With the non-oxidative pathways, the high potential of DMM is no longer restricted to its outstanding combustion characteristics but extended to its production.

Received 5th March 2021,
Accepted 27th April 2021

DOI: 10.1039/d1ee00689d

rsc.li/ees

Broader context

The urgent need for introducing renewable energy into the mobility sector and the low energy density of state-of-the-art batteries call for alternative solutions to meet climate targets. Chemical energy carriers produced from renewable electricity—so called e-fuels—may contribute substantially to such a solution. Oxymethylene ethers (OME_n) are particularly promising as they can not only be produced from carbon dioxide and renewable hydrogen. They can also drastically reduce hazardous emissions during combustion (such as nitrogen oxide and soot emissions) compared to fossil diesel. The commercial production of OME_n is however not sustainable and prevents its broad introduction into the transportation sector. Major inefficiencies are caused by the multitude of involved process steps already towards the first member of OME_n, dimethoxymethane (DMM). To improve process performance, new catalysts have been developed enabling more direct and potentially sustainable pathways for DMM production. In order to evaluate how much these achievements in catalyst development improve sustainability and finally estimate whether DMM can become a sustainable e-fuel—a combined techno-economic analysis (TEA) and life cycle assessment (LCA) of these pathways is inevitable.

^a Process Systems Engineering (AVT.SVT), RWTH Aachen University, Forckenbeckstraße 51, 52074 Aachen, Germany. E-mail: amitsos@alum.mit.edu; Tel: +49 241 80 94704^b Institute of Technical Thermodynamics, RWTH Aachen University, Schinkelstraße 8, 52062 Aachen, Germany^c Institute of Technical and Macromolecular Chemistry, RWTH Aachen University, Worringerweg 1, 52074 Aachen, Germany^d JARA-ENERGY, Templergraben 55, 52056 Aachen, Germany^e Institute of Energy and Climate Research: Energy Systems Engineering (IEK-10), Forschungszentrum Jülich GmbH, Wilhelm-Johnen-Straße, 52425 Jülich, Germany^f Department of Mechanical and Process Engineering, ETH Zurich, Tannenstraße 3, 8092 Zurich, Switzerland

† Electronic supplementary information (ESI) available. See DOI: 10.1039/d1ee00689d



1 Introduction

Greenhouse gas (GHG) emissions from transportation make up about 20% of the global GHG emissions and have been increasing continuously during the past decades. Efficiency improvements have been insufficient to outweigh this increase, which is mainly caused by the growing transportation demand.¹ Additionally, air pollution from transportation has become an increasing cause for health concerns, especially in urban areas. Both aspects motivate the development of transportation options with low emissions based on renewable energy.

One approach to introduce renewable energy into the transportation sector is its direct electrification by battery electric vehicles (BEV). While BEV might be beneficial for short-distance and light-duty transportation,² their wide application-particularly for long-distance and heavy-duty transportation-is questionable in the short- to medium-term.³ For such applications, liquid fuels produced from biomass (biofuels) and/or renewable electricity (e-fuels) can be advantageous due to their comparatively high energy density.

Recently, oxymethylene ethers (OME_n, CH₃O(CH₂O)_nCH₃) have received considerable attention as full substitutes^{4–6} or blend components^{7–10} for diesel fuels. Currently, fossil diesel largely dominates fuel consumption in long-distance and heavy-duty transportation and will maintain its crucial role in the next decades, as highlighted by the International Energy Agency.¹¹ The addressable market for OME_n as a fuel alternative is therefore enormous and ideally complements the one for gasoline fuel alternatives such as ethanol from renewable resources.¹² OME_n can be produced from renewable syngas *via* biomass gasification,^{13–15} or from renewable hydrogen (H₂) and carbon dioxide (CO₂)^{16–20} potentially achieving carbon neutrality over their entire life cycle. Their volumetric energy density (~20 MJ L⁻¹²¹) is about 40% lower than that of diesel, but it is similar to that of other e-fuels²² and about one order of magnitude higher than that of Li-ion batteries for BEV.²³ This makes OME_n particularly suitable for long-distance and heavy-duty transportation. Both OME₁ (methylal or dimethoxymethane, hereinafter referred to as DMM) and OME_{3–5} offer outstanding combustion characteristics (*e.g.*, high thermodynamic efficiency,^{7,9,10} low pollutant emissions^{5,7–10}) but differ in production, infrastructure, and engine compatibility. Whereas OME_{3–5} has more diesel-like properties and can be combusted in conventional diesel engines, DMM needs to be either mixed with additives to gain engine compatibility⁷ or blended with diesel.^{8,24} However, engine modifications seem to remain indispensable for both DMM and OME_{3–5}.^{4,5,25} In addition to the potential direct application in internal combustion engines, DMM is a key intermediate in OME_{3–5} production *via* paraformaldehyde,²⁶ trioxane,^{27,28} or in novel routes *via* gaseous formaldehyde.^{29,30}

Commercial DMM production takes place *via* the condensation reaction of methanol and aqueous formaldehyde (FA).³¹ The major drawback of the underlying reaction pathway is the reaction of H₂ to water during upstream FA production increasing H₂ demand considerably. Moreover, the more water is present in the system, the more undesired side products are formed.³²

To overcome the limitations of commercial DMM production, promising process alternatives have been proposed. A few authors suggest DMM purification *via* extractive^{33,34} and pressure swing distillation³⁵ intending to increase energy efficiency. Other studies propose reactive distillation to shift FA conversion towards DMM³⁶ and combine this approach with pressure swing distillation.³⁷ This combined process concept has been used to develop and analyze the entire process chain for DMM production from renewable H₂ and CO₂.¹⁷ In all of these processes, aqueous FA production still represents a key process step. Although FA production is a highly established and simple process step,²⁶ its exergy efficiency is rather low (73%).¹⁷

The inherent weaknesses of the reaction pathway containing FA production have spurred research activity toward pathways avoiding FA production. Significant improvements in catalyst performance have been achieved³⁸ and novel DMM synthesis pathways proposed (*cf.* Section 2). However, no process concepts have been developed and analyzed so far. Instead, the similar thermodynamic properties of the multi-component system within a novel pathway (the direct reduction of CO₂)³⁹ to those within an established one have been used to estimate the process performance and the impact on climate change of DMM production avoiding FA formation. An increased exergy efficiency of 86% for DMM production from renewable H₂ and CO₂ and the possibility of significant cradle-to-grave CO₂-equivalent emission reductions compared to fossil diesel was reported.²⁰ Given the environmental benefits of DMM and the promising estimates on process performance, the use of more detailed process models in a comparative process analysis alongside the development of novel reaction pathways is essential for sustainable DMM production in the short- to medium-term.

A fair comparison of pathway alternatives is however difficult to perform due to their wide range of technology readiness levels (TRL) and data availability. The comparison of technologies with different TRL has recently received increasing attention, especially in the context of emerging CO₂ utilization technologies.⁴⁰ Comprehensive literature reviews about methods, guidelines, and frameworks for techno-economic analysis (TEA),⁴¹ life cycle assessment (LCA),⁴² and combined TEA and LCA⁴³ dedicated to technologies with varying TRL have recently been published. None of them combines process evaluation based on TEA and LCA with optimization-based process design for technologies with different TRL to explicitly provide feedback for catalyst development.

This article has the major goal to evaluate all reaction pathways from methanol towards DMM in order to provide feedback on the current and prospective process performance for catalyst development. Given the different maturities of the reaction pathways, we introduce a hierarchical process development and evaluation methodology to ensure a fair comparison across these pathways. We perform TEA and LCA on each level to determine the key performance indicators (KPIs) relevant for sustainable e-fuel production. As several pathways are still at an early stage of development, we identify their bottlenecks and derive performance goals that are necessary for process sustainability in the near future.



In Section 2, we summarize all reaction pathways and corresponding key characteristics for DMM production from methanol. Section 3 provides the methodology for process development and evaluation that enables a fair comparison of these pathways. On the basis of the methodology, Section 4 presents the results of the comparison and discusses perspective improvement potential. In Section 5, we conclude our findings.

2 Pathways for DMM synthesis

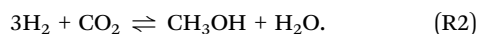
Commercial DMM production is based on the established pathway (Section 2.1), which has been investigated extensively. In contrast, most of the direct pathways (Sections 2.2–2.5) have been proposed recently. Herein, we present the key ideas of these pathways. More detailed information about catalysis and reaction conditions can be found in ESI,[†] Section S1.

2.1 Established pathway

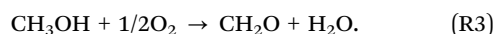
Currently, DMM is produced by the reaction of methanol with (typically aqueous) FA:



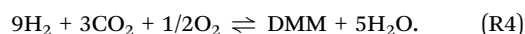
Thus, two intermediates are required: methanol and FA. Methanol can be produced directly from H_2 and CO_2 according to the reaction



FA is typically available as aqueous solution. It is produced from methanol either *via* partial oxidation or *via* combined partial oxidation and dehydrogenation.²⁶ Their overall reaction is



An alternative access to FA is *via* methanol dehydrogenation.⁴⁴ As the process concept for the established pathway intends to represent the state-of-the-art benchmark process for DMM production and methanol dehydrogenation is still at an early stage of development, we do not consider this (potentially beneficial) access to FA for the process concept of the established pathway. All in all, the overall reaction equation starting from H_2 and CO_2 is



2.2 Oxidation of methanol

The direct oxidation of methanol to DMM involves two sequential reactions occurring in the same reactor: *in situ* methanol oxidation to FA and subsequent FA acetalization with methanol to DMM. Both add up to the overall reaction equation



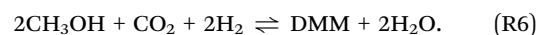
which is identical to the overall reaction equation of the established pathway both starting from methanol (reactions (R1) + (R3)) and starting from H_2 and CO_2 (reaction (R4)). The generated FA from methanol oxidation is directly trapped by methanol to yield DMM, thus avoiding the isolation and

purification of FA. Within this reaction system, the production of one molecule of DMM is accompanied by the formation of two molecules of water (reaction (R5)).³⁸

In contrast to the established pathway, these water molecules are not bound to FA (resulting in methylene glycols), such that the formed water can be more easily removed from the reaction mixture and purged from the process.

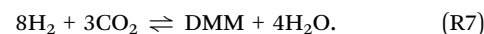
2.3 Reduction of CO_2

The direct reduction of CO_2 to DMM incorporates CO_2 and H_2 into methanol following the overall reaction equation



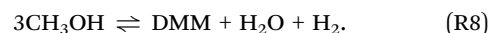
First, methyl formate (MF) is formed by a coupled CO_2 hydrogenation and esterification with methanol. A further hydrogenation step of MF to methoxymethanol (MM) takes place, before a transacetalization with an additional methanol molecule leads to DMM.^{39,45,46}

In contrast to the aforementioned pathways, where FA is produced in a redox-inefficient oxidation step either in a dedicated process step (*cf.* established pathway) or *in situ* (*cf.* oxidative pathway), FA formation is avoided in the reductive pathway. This results in a lower overall H_2 consumption—the main cost driver of e-fuels—following the overall reaction equation starting from H_2 and CO_2



2.4 Dehydrogenation of methanol

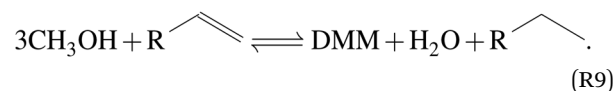
A further non-oxidative pathway for DMM synthesis can be achieved by coupling the dehydrogenation of methanol to FA with the acetalization of FA with methanol:⁴⁷



The prominent advantage of the dehydrogenative pathway is the replacement of the oxidative formation of FA by methanol dehydrogenation leading to the co-formation of valuable H_2 and less water. The produced molecular H_2 can be recycled to the methanol production process leading to the same overall savings in H_2 consumption as for the reductive pathway (*cf.* reaction (R7)). No complex catalyst recycling needs to be realized due to the heterogeneous reaction system. In contrast to the oxidative pathway, the absence of an oxidizing agent further improves operational safety as only gaseous methanol need to be supplied.

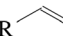
2.5 Transfer-hydrogenation of methanol

Similar to methanol dehydrogenation, methanol transfer-hydrogenation releases one mole H_2 per mole DMM produced following the overall reaction



Starting with three equivalents of methanol, in a first step, the dehydrogenation of one methanol molecule takes place. The (formally) liberated molecular hydrogen is converted *in situ* in



the hydrogenation of a model liquid-organic hydrogen carrier substance (denoted by R ) . Thus, downstream purification of the off gas to access molecular hydrogen is omitted. A subsequent reaction between the FA molecule produced from methanol dehydrogenation and the second equivalent of methanol takes place to form MM. A third equivalent of methanol can then undergo a condensation reaction with MM leading to the desired product DMM.⁴⁸

Similar to the other non-oxidative pathways (reductive and dehydrogenative pathway), the transfer-hydrogenation of methanol toward DMM benefits from the same savings in overall H_2 consumption (*cf.* reaction (R7)). These savings are enabled by a beneficial H_2 management *via* the regeneration of H_2 from its carrier substance and its recycling.

3 Process design and evaluation accounting for TRL

The TRLs of the DMM reaction pathways differ significantly, and so does the data availability for process design and evaluation: Whereas the established pathway has been investigated extensively over the last three decades (Section 2.1), the majority of direct DMM pathways has been discovered during the last years (Sections 2.2–2.5). To still ensure a fair comparison despite the different stages of development and to ultimately lead the way towards sustainable DMM production, we introduce a hierarchical process development and evaluation methodology (Fig. 1). Within this methodology, process development (Section 3.1) and evaluation (Section 3.2) take place on up to three hierarchy levels depending on the data availability for each considered pathway. On Level 1, only reaction equations are required for calculating the maximum pathway potential. On Level 2, thermodynamic data and at least experimental data on reactions showing a sufficiently high performance need to be available to develop first process concepts. On Level 3, more detailed models are required for process optimization. On each level, three KPIs are calculated: process efficiency, production cost, and impact on climate change. We use these performance indicators to derive pathway-specific feedback for catalyst development to effectively benefit from both process and catalyst development (Section 4.4).

By applying the methodology to each pathway, we attain two important achievements: First, the pathways become comparable

up to their highest common level despite their discrepancies in maturity. A fair comparison is ensured by using the same boundary conditions, model detail, and input data. Second, the gradual refinement of models and input data throughout the levels reveals information about the most relevant parameters and the gap between current and highest possible process performance. This information is not only essential for process optimization but also for catalyst optimization.

3.1 Process development

We develop the process for each pathway sequentially from Level 1, containing only the most essential pathway characteristics, up to Level 3, containing enough information about the process for process optimization using rigorous models. In this section, we explicitly distinguish between levels, because the models and methods used for process development differ significantly between levels. Each level addresses an individual question:

- Level 1: What is the maximum potential of the pathway?
- Level 2: Which performance can we expect from a corresponding process?
- Level 3: What is the actual performance of an optimized process?

Level 1. Pathway potential. On Level 1, we model the process as a black-box containing only the stoichiometric coefficients of the desired reaction, thus assuming perfect selectivity. To calculate the maximum potential of the pathway, we further assume ideal separation and the recycling of unreacted educts, valuable intermediates, and side products. The result and key input for pathway evaluation on this level is the DMM-specific minimum raw material consumption.

Level 2. Process concept. On Level 2, we develop the separation system and the recycle structure with the reactor as the central unit of the process. To determine the distillation sequence, we follow a process synthesis framework for the design of distillation processes from the literature.⁴⁹ Herein, we generate multiple variants which we then evaluate based on the Rectification Body Method (RBM).⁵⁰ Heat integration by a subsequent pinch-analysis of the entire process finally enables finding the least energy-intensive process for each pathway. On this level, we consider experimental data on reaction performance (Table S1, ESI†) or, if already available, reaction kinetics, and nonideal thermodynamics for all pathways (Tables S2–S4, ESI†). We use the process simulator Aspen Plus v11 to calculate mass balances and the energy demand for feed compression, and the in-house tool EE-ToolBox⁵¹ (incorporates the RBM) to calculate the minimum energy demand (MED) of each distillation task.

Level 3. Optimized process. On Level 3, we extend the model of the process with the lowest MED from Level 2 with additional compressors and pumps, and replace the RBM with detailed tray-to-tray distillation models.⁵² This does not only increase accuracy, but also enables a more detailed process design and column sizing. We optimize the process in such a way that operational expenditure (OPEX) and capital expenditure (CAPEX) are minimized simultaneously. This results in a complex mixed-integer nonlinear programming (MINLP) problem. As currently global solution seems intractable, we follow a successive

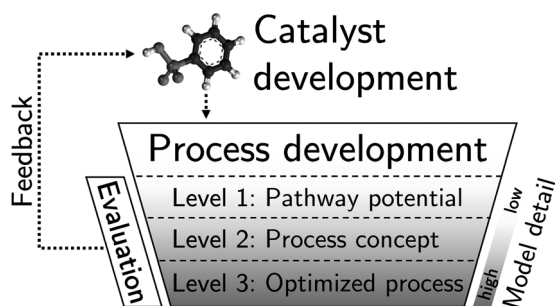


Fig. 1 Hierarchical process development and evaluation methodology.



initialization procedure, reformulate the MINLP problem into a sequence of nonlinear programming (NLP) problems, and handle the flash calculations hidden from the numerical solver.⁵² During optimization, only the purity constraints of streams leaving the process are considered. This prevents decisions on the sharpness of intermediate separation splits (particularly relevant for azeotropic distillation) and thus preliminary heuristic decisions. We perform the optimization with the algebraic modeling system GAMS using SNOPT as numerical solver and external functions for thermodynamic calculations.⁴⁹

3.2 Pathway evaluation

The results obtained on each level in process development (*cf.* Section 3.1) are inputs for the pathway evaluation. In accordance with the levels considered for process development, we evaluate each pathway up to their highest level always considering the three KPIs: process efficiency, production cost, and impact on climate change. The analyses between levels are dependent from one another only in such a way that the optimized process on Level 3 results from the least energy-intensive process concept on Level 2. The evaluation models and methods are the same for each level and differ only in their input data (*cf.* Table S5, ESI[†]).

Efficiency model for DMM processes. Since renewable electricity dedicated to e-production (nonconventional production of commodities, fuels, or heat using processes that predominantly utilize renewable electricity⁵³) will remain limited in the short- to medium-term, process efficiency is one of the KPIs for e-fuel production. In the present work, we consider exergy efficiency to restrict the energy output of the system to energy that is actually usable. Exergy efficiency is the maximum amount of useful energy that leaves the process (through the product, side products, and excess heat) relative to the amount of useful energy that enters the process (through H₂, CO₂, heat demand, and electricity). Process exergy efficiency $\eta_{P,l}$ is calculated by

$$\eta_{P,l} = \frac{\dot{E}_{DMM} + \dot{E}_{side} + \dot{E}_{Q_{out}}}{\dot{E}_{H_2} + \dot{E}_{CO_2} + \dot{E}_{Q_{in}} + P_{feed} + P_{misc}} - 1 \in \{L1, L2, L3\}, \quad (1)$$

where \dot{E}_{DMM} , \dot{E}_{side} , \dot{E}_{H_2} , and \dot{E}_{CO_2} is the DMM-specific thermomechanical and chemical (based on higher heating value (HHV)) exergy content of DMM, side products, H₂, and CO₂, respectively; $\dot{E}_{Q_{out}}$ and $\dot{E}_{Q_{in}}$ is the DMM-specific exergy of excess heat and heat demand of the process, respectively ($T_{ambient} = 298.15$ K); and P_{feed} and P_{misc} is the DMM-specific electricity demand for feed compression and miscellaneous compression and pumping within the

entire process, respectively. We distinguish between two types of exergy efficiency: process exergy efficiency (*cf.* eqn (1)) and system exergy efficiency (*cf.* eqn (S2), ESI[†]). Process exergy efficiency refers only to the process for DMM production from H₂ and CO₂, thus decoupling the provision of raw materials from the process. In contrast, system exergy efficiency refers to the entire system including the provision of raw materials. For the provision of raw materials, we consider a best and a worst case scenario (Table 1). In the best case scenario, H₂ is provided by a solid oxide electrolyzer cell (SOEC) and CO₂ is provided by a high purity (~100%) industrial point source. In the worst case scenario, H₂ is provided by a polymer electrolyte membrane (PEM) electrolysis and CO₂ is provided by direct air capture (DAC). The parameters for the best and worst case scenario are summarized in Table S8 (ESI[†]).

Economic evaluation method for DMM processes. For an economic evaluation, we consider both OPEX and CAPEX. OPEX constitutes costs for raw materials (H₂ and CO₂), steam, coolants, and electricity. CAPEX constitutes investment costs for distillation columns (shell, trays, condensers, reboilers), reactors, pumps, and compressors. Costs for catalysts and heat exchangers are excluded as the catalysts for the direct pathways are not commercially available yet and no heat exchanger network is developed. On the most detailed level, we further calculate cost of manufacturing (COM) to get a clearer representation of a possible market price for DMM. The type and amount of output data on each level define the costs to include in the economic evaluation on each level (Table S5, ESI[†]). Production cost is measured in \$ L_{diesel-eq.}⁻¹. For the economic evaluation, we analyze the influence of the most relevant parameters by a sensitivity analysis. All equations and parameters are summarized in Section S3.2 (ESI[†]).

LCA method for DMM processes. LCA is a standardized method (ISO 14040/14044^{54,55}) for evaluating potential environmental impacts of product systems. It considers the entire life cycle of a product system from raw material extraction until waste disposal ('cradle-to-grave').⁵⁶ All environmental impacts of the material and energy flows that are exchanged with the environment are characterized in LCA.

The goal of this study is to compare DMM pathways from a climate point of view. As DMM intends to substitute fossil fuels particularly in long-distance and heavy-duty transportation, we also include fossil diesel to this comparison. Due to the different combustion characteristics of these two fuels, we consider their combustion at the end-of-life to cover the cradle-to-grave perspective. The functional unit "the provision

Table 1 Selected technologies for the best and worst case scenario for the evaluation of DMM pathways. Parameters, references, and datasets are summarized in Tables S8–S10 (ESI)

	Best case scenario	Worst case scenario
H ₂ provision	SOEC	PEM electrolysis
CO ₂ provision	Ideal point source	DAC
Electricity	Onshore wind park (Germany)	Power grid mix today (Germany)
Heat ($T < 90$ °C)	Heat pump	Steam
Heat (90 °C $< T < 250$ °C)	Electrode boiler	Steam
Heat ($T > 250$ °C)	Electrode boiler	Natural gas boiler
Cooling		Vapor compression refrigeration system



of 1 MJ of enthalpy of combustion" for both DMM and fossil diesel enables a consistent comparison between the investigated product systems. To ensure consistency also with the TEA, we do not consider environmental credits (so-called avoided burdens, *i.e.*, an environmental credit to account for the avoided burden of the conventional production) for co-produced side products (MF and dimethyl ether (DME)) and heat. The influence of these avoided burdens on the climate impact of DMM is however investigated in Section S6 (ESI†). We focus on the impact category climate change (heat radiation absorption of the atmosphere caused by anthropogenic emissions, measured in kg of CO₂-equivalents⁵⁷) as e-fuels mainly aim at reducing the climate impact of transportation. For a holistic assessment of DMM, further impact categories are also important but beyond the scope of this work. The same best and worst case scenarios as for the exergy efficiency analyses are used and extended according to Table 1. All assumptions and datasets are summarized in ESI†, Section S3.3.

4 Results on key performance indicators for DMM production

On the basis of the models and assumptions presented in Section 3, each pathway is analyzed up to a certain level given their data availability. Thermodynamic data is available for all considered pathways in open literature (*cf.* Section 3.1). In contrast, reaction data differs significantly between pathways. For the established pathway, reaction kinetics are available^{58,59} and enable the propagation of the pathway through all three levels. For the oxidative pathway, a comprehensive experimental data base on reaction performance has been accumulated,³⁸ yet

a kinetic model has not been derived. Notwithstanding, the vast amount of data makes the propagation through all three levels possible. For the reductive pathway, considerable achievements in catalyst optimization^{39,46} and the successful application of an alternative catalytic system⁴⁵ make process development and evaluation on Level 2 possible. For process optimization on Level 3, however, a more extensive data base or (ideally) reaction kinetics are required. For the dehydrogenative pathway, only little experimental data has been reported.⁴⁷ Nevertheless, the achieved reaction performance is high enough to develop a first process concept on Level 2. For the transfer-hydrogenative pathway, turnover numbers (TON) of the same magnitude as for the reductive pathway have been reported.⁴⁸ A low catalyst loading compared to the reductive pathway however results in lower DMM single-pass yields with respect to methanol. Thus, the evaluation of a process concept for the transfer-hydrogenative pathway on Level 2 would systematically underestimate its performance.

On the basis of these classifications, we developed process concepts for the reductive and dehydrogenative pathway (Fig. 2) following the procedure presented in Section 3.1. For the established and oxidative pathway, we adapted processes from the literature^{17,60} and calculated corresponding mass and energy balances (Tables S11–S13, ESI†) for the analyses on both Level 2 and 3.

In the following, we present the results of the analyses structured by KPI to highlight both how they differ between pathways and how they evolve through the levels for each pathway.

4.1 Exergy efficiency

On Level 1, we show that the benefit of the lower stoichiometric H₂ consumption for the reductive, dehydrogenative, and transfer-hydrogenative pathway corresponds to an increase in process

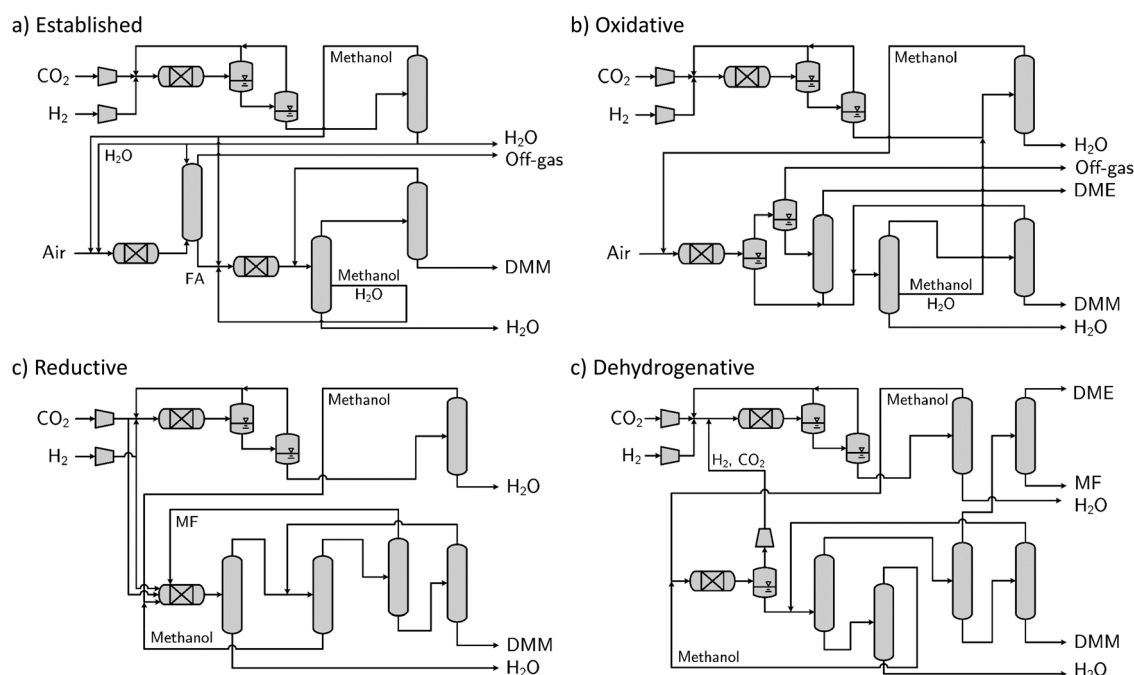


Fig. 2 Process concepts for all considered pathways on Level 2. All possible distillation sequences have been screened and the least energy-intensive sequence has been chosen.



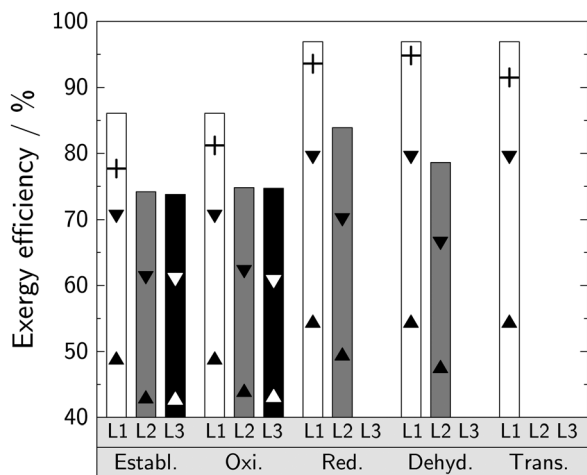


Fig. 3 Exergy efficiencies for all evaluated levels and pathways. The bars correspond to the process exergy efficiency (DMM production starting from H_2 and CO_2), whereas the triangles correspond to the best (\blacktriangledown) and worst (\blacktriangle) case scenario for the system exergy efficiency (DMM production starting from electricity, water, and a CO_2 source). The two scenarios are specified in Table 1. The crosses correspond to Level 1 evaluations considering the experimental selectivities of the entire value chain instead of perfect selectivity.

exergy efficiency of 11% (Fig. 3). These non-oxidative pathways consume 8 mol H_2 per 1 mol DMM formed instead of 9 mol H_2 (established and oxidative pathway). The benefit of saving 1 mol H_2 per 1 mol DMM produced enables a maximum process exergy efficiency of almost 97%. A comparison with the maximum process exergy efficiency of other e-fuels (ethanol: 90%; methanol: 95%; methane: 83%; DME: 97%; all based on HHV) and their higher stoichiometric H_2 consumption relative to their heating values (Table S14, ESI[†]) demonstrate the great potential of the non-oxidative DMM reaction pathways. Considering the experimental selectivities of the entire value chain on Level 1 instead of perfect selectivity, the gap between experimental exergy efficiencies and their theoretical limit become clear (Fig. 3). The negative effects caused by a low reaction conversion, however, is captured only by Level 2 and 3 evaluations.

On Level 2, by considering the actual reaction performance from lab-scale experiments or pilot plants (Table S1, ESI[†]) and process concepts (*cf.* Fig. 2), the exergy efficiency decreases significantly for all pathways. One common reason for this decrease is that up to 6% of the exergy content of DMM is required for H_2 and CO_2 feed compression to maximum operating pressures of 70 to 80 bar. Furthermore, main exergy losses in the established pathway are due to methanol combustion in the FA process step¹⁷ and a comparably low overall carbon-based DMM yield (90%). The overall carbon-based DMM yield of the oxidative pathway (94%) is considerably higher and only little external heating is required (*cf.* Table S13, ESI[†]). Yet, exergy efficiency is only about the same as that of the established pathway, because the product removal from a highly diluted gaseous reactor effluent requires more than 5% of the DMM exergy. The overall carbon-based DMM yield of the reductive pathway (97%) is even higher than that of the oxidative pathway

as the only reported side product is the intermediate MF and assumed to be recycled back into the reactor. However, a relatively low methanol conversion of 10% results in high recycle streams and a high heat demand for separation (8% of the DMM exergy). This bottleneck—the most relevant one of the reductive pathway—has not been captured by the process estimations in preceding studies, where process efficiency has been overestimated (86%).²⁰ The methanol conversion of the dehydrogenative pathway is only 3.6%, thus resulting in a six times higher methanol recycle stream compared to the reductive pathway and in a heat demand for product separation of 16% of the DMM exergy. This increased heat demand reduces exergy efficiency considerably. Also the overall carbon-based DMM yield of the associated process is significantly lower (77%) as MF and small amounts of DME are formed as side products. In contrast to the reductive pathway, MF can not be converted further to DMM in the dehydrogenative pathway. As MF and DME are valuable side products, the comparatively low DMM selectivity has only negligible effect on exergy efficiency.

On Level 3, the exergy efficiency of both the established and oxidative pathway do not differ significantly from those of Level 2. Performance gains due to optimization are balanced by accounting for more detailed models (*e.g.*, tray-to-tray distillation models) and the power demand for additional process units (*e.g.*, pumps and compressors for recycle streams). However, we still benefit from the analyses on Level 3 in two ways: First, we obtain information on equipment sizing, which enables costing. Second, we gain more reliability on the results as more rigorous models are used. These two outcomes are highly relevant for industrial implementation.

4.2 Production cost

As is typical for e-fuels, the H_2 price dominates DMM production cost for all pathways and levels (Fig. 4).

On Level 1, the analyses reveal that the H_2 savings of the non-oxidative pathways correspond to cost reductions of 11% of total raw material costs. As transportation is highly price sensitive, these savings in H_2 consumption are paramount for DMM production.

On Level 2, an imperfect selectivity toward DMM results in additional costs. These are most pronounced for the dehydrogenative pathway due to the significant co-production of MF and DME, for which we do not consider a monetary credit given the lack of reliable data. For this pathway, also the costs for steam are the highest among the pathways due to its low methanol conversion (*cf.* Table S1, ESI[†]) and thus high recycle streams. Whereas conversion improvements by catalyst modifications (*cf.* Section 4.4) are limited by the chemical equilibrium of the dehydrogenative pathway, process modifications have potential to elevate equilibrium conversion. For instance, membrane reactors with molecular-sieves can be used for selective and *in situ* H_2 removal.⁶⁷ This might increase methanol conversion and reduce DMM production cost significantly. With the currently achievable reaction performance, however, the burdens of the dehydrogenative pathway result in considerably higher DMM production cost compared to other e-fuels (methane, methanol, and DME), which were evaluated on Level 2 using the



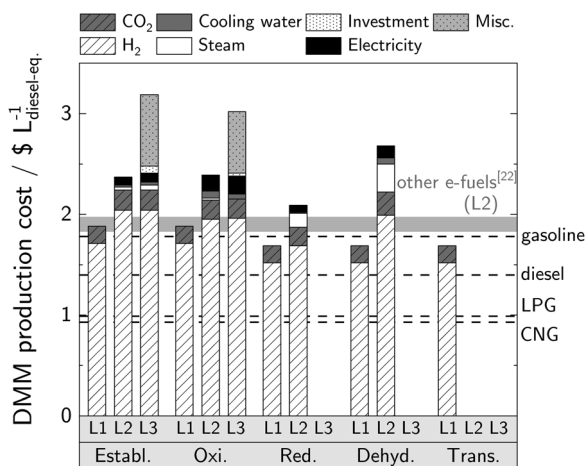


Fig. 4 Production cost for each synthesis route for all evaluated levels. Perspective H_2 and CO_2 prices of $5\text{ \$ kg}^{-1}$ ⁶¹ and $70\text{ \$ t}^{-1}$ ⁶² are considered for PEM electrolysis and CO_2 capture from post-combustion, respectively. A price of $7.78\text{ \$ GJ}^{-1}$ for steam at 160 °C ,⁶³ $0.02\text{ \$ t}^{-1}$ and $1.2\text{ \$ t}^{-1}$ for cooling water at 25 °C and 5 °C , respectively,⁶⁴ and $2.40\text{ \$ t}^{-1}$ for refrigeration at -35 °C ⁶⁴ are considered. Investment cost and all miscellaneous costs are calculated after Guthrie⁶⁵ and Turton *et al.*,⁶⁶ respectively. Corresponding cost parameters can be found in Section S3.2 (ESI†). The production cost of other e-fuels refer to methane, methanol, and DME and correspond to the assumptions and model detail on Level 2.²² The consumer prices of the conventional fossil fuels gasoline, diesel, LPG, and CNG include all taxes.

same boundary conditions and model depth.²² In contrast, production cost *via* the reductive pathway are in the same range as that of other e-fuels already with the current catalyst and can be further reduced by an optimized reactor design and/or co-solvent facilitating the dissolution of H_2 and CO_2 into the reaction phase. For the oxidative pathway, the product removal from the gaseous reactor effluent by a refrigeration machine causes the highest electricity costs among the pathways and should be avoided in an industrial application. Therefore, the application of a less energy-intensive unit operation for product removal (*e.g.*, adsorption) need to be investigated in future work to further reduce DMM production cost. Beyond that, the product dilution in the reactor effluent can be reduced by using pure oxygen from the electrolyzer instead of air for the oxidation reaction. An increased product concentration in the reactor effluent would directly reduce energy demand for product purification.

On Level 3, the economic evaluation for the established and oxidative pathway shows that investment cost for the DMM plant can be neglected (less than 1%) considering a plant life time of 10 years. It is important to note, however, that investment cost for the electrolyzer are considered in the H_2 price already. The consideration of miscellaneous costs on Level 3 results in an increase of production cost of about 20% compared to Level 2 for the established and oxidative pathway. As these costs mainly constitute general manufacturing expenses (*cf.* Turton *et al.*⁶⁶), a similar increase is expected for the non-oxidative pathways.

The H_2 price is the largest cost driver for DMM production having a major influence on whether an e-fuel like DMM will

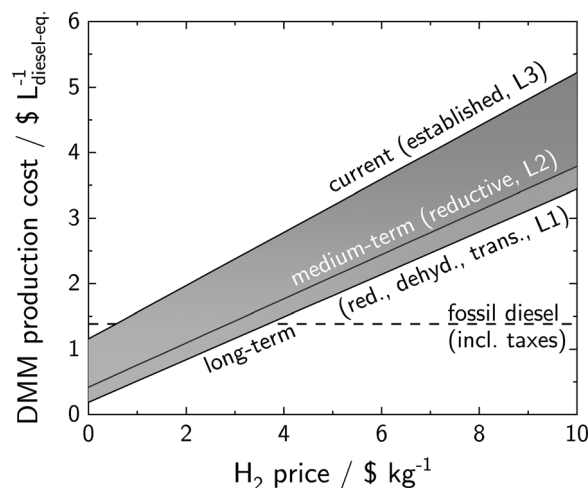


Fig. 5 DMM production cost dependence on H_2 price. The base case CO_2 price is $70\text{ \$ t}^{-1}$.⁶²

become a relevant contributor in a future mobility concept or not. Unfortunately, it is also one of the most uncertain ones, which makes an analysis of its influence on DMM production cost indispensable.

Fig. 5 reveals clearly: only at low H_2 prices (below $3.7\text{ \$ kg}^{-1}$), DMM has the chance to become cost competitive with its main competitor fossil diesel. For the extensive application of DMM in individual transportation, where fuel acceptance is driven by fuel cost,⁶⁸ a competitiveness with cheap fossil diesel and thus low H_2 prices might be an essential precondition. The target consumer price of DMM should therefore lie within the region of the consumer price of fossil diesel ($1.4\text{ \$ L}^{-1}$). Without the non-oxidative pathways, DMM production cost will hardly fall below this target price as H_2 prices would need to fall below $0.5\text{ \$ kg}^{-1}$ for the established pathway.

In terms of CO_2 supply, the technology for CO_2 provision determines whether CO_2 contributes significantly to DMM production cost or not. Considering industrial point sources for CO_2 provision ($0\text{ \$ t}^{-1}$ to $200\text{ \$ t}^{-1}$,⁶² Fig. S1, ESI†), the share of CO_2 on total DMM production cost is comparably low. Technologies with a higher cost for CO_2 capture (*e.g.*, $600\text{ \$ t}^{-1}$ for DAC⁶⁹) may however become a limiting factor for a successful implementation of DMM in a future mobility concept.

4.3 Impact on climate change

The results of the LCA for the best case scenario show clearly: If renewable electricity for DMM production is used exclusively (according to the power-to-X concept⁵³), the cradle-to-grave impact on climate change of DMM does not differ significantly between pathways and levels (Fig. 6). Compared to that of fossil diesel ($86\text{ g}_{\text{CO}_2\text{-eq.}}\text{ MJ}^{-1}$), all pathways for DMM production enable considerable $\text{CO}_2\text{-eq.}$ emission reductions.

For the worst case scenario, the impact on climate change of the different routes is in the range of $350\text{ g}_{\text{CO}_2\text{-eq.}}\text{ MJ}^{-1}$ to $550\text{ g}_{\text{CO}_2\text{-eq.}}\text{ MJ}^{-1}$ and, by this, exceeds that of fossil diesel considerably. With the current German electricity mix,⁷⁰ it is therefore not climate friendly to produce and use DMM as an



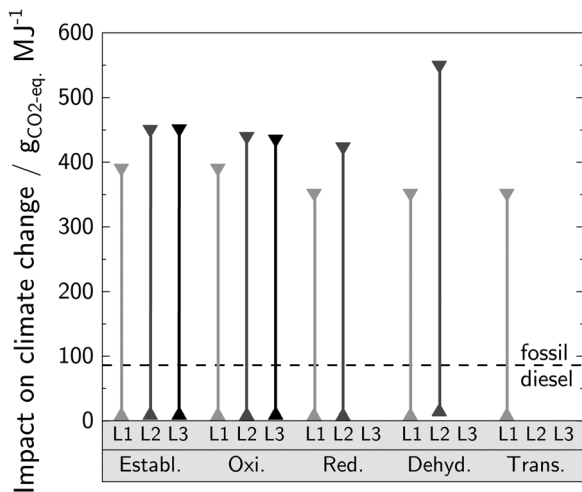


Fig. 6 Ranges of cradle-to-grave impact on climate change of different DMM synthesis routes. The routes are evaluated on different levels for both the best (▲) and worst (▼) case scenario and are compared to fossil diesel. The functional unit is "the provision of 1 MJ of enthalpy of combustion". The combustion of the co-products MF and DME at their end-of-life is included for the dehydrogenation and oxidative route on Level 2 and 3 to cover the cradle-to-grave perspective. The two scenarios are specified in Table 1.

alternative to fossil diesel. The different impacts on climate change between the pathways and levels are caused by the same reasons as those for the differences in exergy efficiencies (*cf.* Section 4.1). A detailed contribution analysis for both the best and worst case scenario are presented in Fig. S2 and S3 (ESI[†]), respectively.

From the analyses of the worst and best case scenario regarding the impact on climate change of DMM, we can draw two main conclusions: First, the carbon footprint of electricity supply needs to be low as cradle-to-grave CO₂-eq. emissions of DMM exceed those of fossil diesel considerably if the current German electricity mix is utilized. Second, the higher the carbon footprint of the electricity mix is, the more important becomes the choice for the pathway in order to yield a low impact on climate change of DMM.

Fig. 7 therefore shows the impact on climate change of DMM for the different pathways on Level 2 as a function of the impact on climate change of electricity supply. The intersections of the graphs with the solid black line are the break-even points, where the CO₂-eq. emissions of DMM fall below those of fossil diesel. The impact on climate change of the reductive DMM pathway depends the least on that of the electricity supply. Below the break-even point of 190 gCO₂-eq. kW h⁻¹, DMM produced by the reductive pathway is more favorable compared to fossil diesel. This break-even point has a rigorous bound at about 225 gCO₂-eq. kW h⁻¹ (Fig. S4, ESI[†]). At this bound, only stoichiometric H₂ and CO₂ consumption is considered (Level 1) such that no process can exceed this bound. The established and oxidative pathways have a break-even point of 170 gCO₂-eq. kW h⁻¹ and are thus less favorable compared to the reductive pathway. For these three pathways, the grid mixes of Norway, France, and in contrast to DMM/fossil diesel blends with 35 vol% DMM,²⁰ also of Switzerland and Finland, are

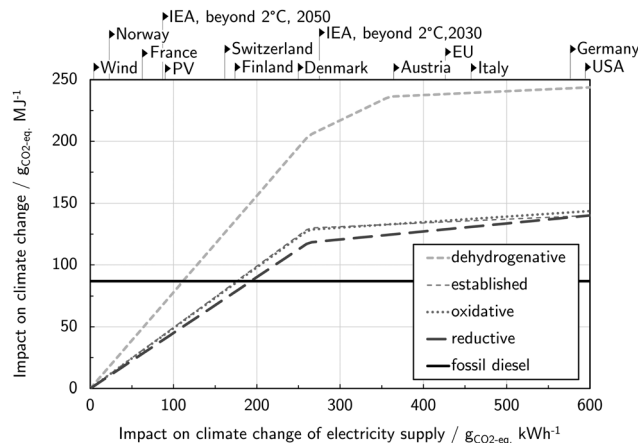


Fig. 7 Sensitivity of the cradle-to-grave impact on climate change of DMM with respect to the impact on climate change of electricity supply for different DMM synthesis pathways on Level 2 and fossil diesel. The impact on climate change is calculated using the current catalyst performance of each pathway. Avoided burdens for co-produced MF, DME, and excess heat are not considered. Below 360 gCO₂-eq. kW h⁻¹, heat between 90 °C to 250 °C is provided by electrode boilers instead of steam production (relevant only for the dehydrogenative pathway). H₂ is supplied by SOEC instead of conventional steam methane reforming below 260 gCO₂-eq. kW h⁻¹. At lower carbon-intensities of electricity supply, both the electrode boilers and the SOEC allow for lower climate change impacts compared to their conventional counterparts. The solid black lines at the top of the graph represent the impact on climate change of country-specific grid mixes and two forecasts for the global grid mix of 2030 and 2050 that are based on the "beyond 2 °C scenario" of the International Energy Agency.⁷¹

sufficient for producing and using neat DMM with less impact on climate change than fossil diesel already today. In this range, it does matter which pathway is used for DMM production from a climate impact perspective. The carbon footprint of the dehydrogenative pathway depends most strongly on the impact on climate change of electricity supply as the selectivity towards DMM is the lowest. The co-production of MF and DME requires additional electricity and the low methanol conversion results in a high heat demand for product separation (*cf.* Tables S11–S13, ESI[†]). The impacts on climate change evaluated on Level 1 and 3 are presented in Fig. S4 and S5 (ESI[†]), respectively.

4.4 Catalyst improvement potential

The non-oxidative pathways have been proposed just recently and may offer catalyst improvement potential that has not been captured with the analyses on Level 2 so far. To consider this improvement potential, we analyze the theoretically achievable reaction performance of the reductive, dehydrogenative, and transfer-hydrogenative pathway by assuming restricted equilibrium conversion. Restricted equilibrium considers only the desired reaction (perfect DMM selectivity).⁷² We calculate the equilibrium DMM yield using the stoichiometric chemical and phase equilibrium (REquil reactor model in Aspen Plus v11) and evaluate the current gap to this performance. We then use these theoretical reaction conditions to evaluate the maximum process efficiency, minimum production cost, and minimum impact on climate change on Level 2 for all non-oxidative pathways.



Reductive pathway. Reaction equilibrium calculations show that DMM yield increases strongly with decreasing temperature due to the exothermic nature of reaction (R6) (Fig. 8a). Experimental DMM yields confirm this trend in the temperature range of 80 °C to 120 °C, but they are well below equilibrium yield due to catalyst deactivation during the course of reaction. In the temperature range below 80 °C, experimentally observed DMM yields decrease significantly since the used catalyst requires a certain activation energy to convert CO₂ and H₂. To exploit the increased DMM equilibrium yield at temperatures below 80 °C, catalysts requiring even lower temperatures and thus lower activation energies for CO₂ activation are necessary. In terms of reactor pressure, the DMM equilibrium yield increases linearly with increasing pressure (Fig. S6, ESI†). Experiments do not confirm this linear trend so far, which could be caused by limitations of the experimental set-up. Due to the minimum temperature of 80 °C required for catalyst activity and the independence of experimental DMM yield on pressure, we choose an optimal operating point of 80 °C and 80 °C for evaluating the maximum performance of the reductive pathway on Level 2. This corresponds to an equilibrium yield of 15.7% and an improvement of 7.4 percentage points compared to the current state of the catalyst.

At equilibrium yield, the heat demand required for product separation is reduced by 81% compared to the current state of the catalyst (Tables S17 and Fig. S7, ESI†). As the heat demand of the reductive pathway causes the main exergy losses, this reduction is highly beneficial and increases exergy efficiency by 5 percentage points to an overall process efficiency of 89%. Production costs are reduced by only 0.1\$ L_{diesel-eq.}⁻¹ as fossil-based heating is cheap compared to renewable H₂. A major benefit in reducing fossil-based heating rather lies in associated CO₂-eq. emission reductions, which are about 10% (44 g_{CO₂-eq.} MJ⁻¹) in the worst case scenario. The best case scenario utilizes almost CO₂-neutral heating sources, such that a reduced heat demand has only a negligible effect on climate impact (Fig. S10, ESI†).

Dehydrogenative pathway. The experimental data on the dehydrogenative pathway demonstrates that the maximum experimentally achieved DMM yield (4.1%) is 10⁴ times higher than that if no side reactions would be suppressed.⁴⁷ This corresponds to 48% of the DMM equilibrium yield at 240 °C (Fig. 8b). At higher temperatures, equilibrium DMM yield increases, but DMM selectivity decreases due to elevated FA and MF co-production.⁴⁷ However, co-produced FA and unreacted methanol can be converted to DMM (*cf.* Section 2.1) in an additional reactive distillation section,³⁷ such that the overall DMM yield does not necessarily decrease with increasing temperature. To still benefit from rather mild reaction conditions and maintain high yields, we chose an equilibrium DMM yield at 300 °C (9.8%) for analyzing potential process improvements by further catalyst development. Reaction pressure does not have a significant influence on DMM yield and is kept constant at 1 bar.

Similar to the reductive pathway, heat demand decreases by about 80% at equilibrium yield at 300 °C and exergy efficiency increases by 6 percentage points to an overall process efficiency of 85% (Table S17 and Fig. S8, ESI†). The maximum cost reduction potential is 0.6\$ L_{diesel-eq.}⁻¹ or 22% of the production costs considering the current state of the catalyst. This reduction is enabled mainly by the assumed perfect selectivity (0.3\$ L_{diesel-eq.}⁻¹) and by the lower heat demand (0.2\$ L_{diesel-eq.}⁻¹). As the absolute reduction in heat demand is even higher than that of the reductive pathway, the associated reduction in CO₂-eq. emissions in the worst case scenario is higher as well (26% or 140 g_{CO₂-eq.} MJ⁻¹). Although the best case scenario utilizes almost CO₂-neutral heating sources, significant CO₂-eq. emission reductions can be achieved there as well due to the higher selectivity (*cf.* Fig. S10, ESI†).

Transfer-hydrogenative pathway. For the transfer-hydrogenative pathway, no process concept has been developed on Level 2, because reported DMM yields are still low (Table S1, ESI† and Fig. 8c). The low DMM yields are mainly caused by comparatively low catalyst concentrations used in the experiments, which makes

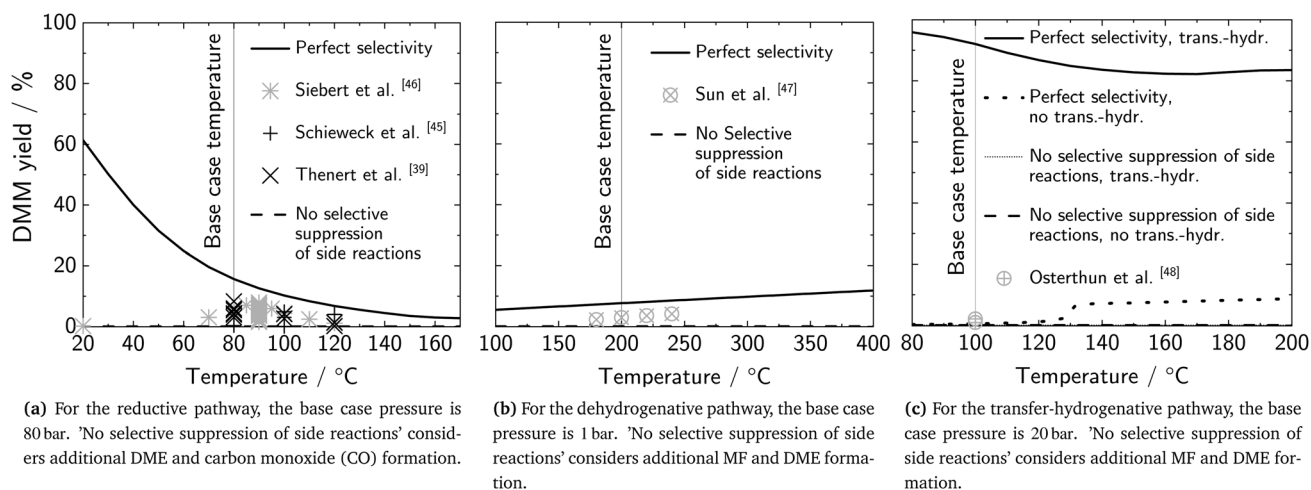


Fig. 8 DMM yield dependence on reactor temperature for the reductive pathway (a), the dehydrogenative pathway (b), and the transfer-hydrogenative pathway (c). Restricted equilibrium conversion (considering perfect DMM selectivity) has been considered throughout the entire temperature range and was calculated with an REquil reactor model in Aspen Plus v11.



the direct comparison between the pathways difficult. The maximum potential calculations can overcome these difficulties and allow also for the transfer-hydrogenative pathway a fair comparison with its alternatives from a process perspective.

The equilibrium reaction calculations reveal that experimentally achieved DMM yields (up to 2.1%) are well below restricted equilibrium conditions (92.1%) at 100 °C assuming the concurrent transfer-hydrogenation reaction of styrene to ethylbenzene (EB) (Fig. 8c). Whereas the experimentally achieved maximum selectivity is almost perfect (98.2%), methanol conversion is still low (0.9%). Without the H₂ removal by the transfer-hydrogenative reaction ('no trans-hydr.' in Fig. 8c), equilibrium yield would be limited to only 0.3%, which is about one third of the experimentally achieved yield. The strong effect of *in situ* H₂ removal on DMM yield for the transfer-hydrogenative pathway indicates similar benefits for the dehydrogenative pathway and should therefore be investigated in future research. Irrespective of a concurrent transfer-hydrogenation reaction, if the catalyst would not suppress MF and DME formation selectively, no DMM would be formed but exclusively MF and DME with selectivities of 83.1% and 16.9%, respectively.

To evaluate the maximum potential of the transfer-hydrogenative pathway, we assume equilibrium yield at 100 °C (92.1%) and the concurrent transfer-hydrogenation of styrene to EB. In contrast to the other non-oxidative pathways, the evaluated process concept for the transfer-hydrogenative pathway contains the following additional steps: the transfer-hydrogenation of styrene, the subsequent removal of its hydrogenated molecule EB, the dehydrogenation back to styrene and H₂, and the recycling of styrene into the reactor. The resulting process concept and model assumptions are given in ESI,† Fig. S13.

If EB dehydrogenation and H₂ recycling is considered at no cost (decoupling the pathway evaluation from the choice of the model hydrogen carrier substance), a maximum process exergy efficiency of 91% can be achieved (Fig. S12a, ESI†). This is slightly higher than that of the reductive pathway (89%) and significantly higher than that of the dehydrogenative pathway (85%) due to a higher equilibrium conversion and, in turn, a lower heat demand. Considering commercial EB dehydrogenation and H₂ recycling, the efficiency drops to 72% due to its massive heat demand at high temperature (*cf.* Table S17, ESI†). It should be noted that the use of styrene as a hydrogen acceptor is not industrially viable, since styrene itself is produced industrially by EB dehydrogenation. The hydrogen carrier couple styrene-EB was nevertheless selected for the experiments due to its ease of hydrogenation and analytical simplifications in the experimental development of a transition-metal catalyst that could catalyze the conversion of methanol to DMM. For industrial applications, a hydrogen carrier couple allowing for a more energy efficient H₂ recycling has to be found, which is subject to ongoing research. Alternatively, the co-production of a high value hydrogenated by-product could be envisioned as well.

The minimum production cost for the transfer-hydrogenative pathway is identical to that of the reductive pathway ($2.0\$ L_{\text{diesel-eq.}}^{-1}$) (Fig. S12b, ESI†). The same amount of H₂ and CO₂ is consumed as well as compressed to operating pressure. DMM production cost by the dehydrogenative pathway is slightly more expensive

($2.1\$ L_{\text{diesel-eq.}}^{-1}$) as a considerable amount of external heat is required for product separation despite equilibrium conversion.

In terms of impact on climate change, the transfer-hydrogenation pathway has the lowest climate impact among the alternative pathways in the worst case scenario ($370 \text{ g}_{\text{CO}_2\text{-eq.}} \text{ MJ}^{-1}$) if EB dehydrogenation and H₂ recycling at no cost is considered (Fig. S12c, ESI†). In the other cases, the climate impact slightly exceeds that of the dehydrogenative pathway. For the best case scenario, the impact on climate change is below $10 \text{ g}_{\text{CO}_2\text{-eq.}} \text{ MJ}^{-1}$ and thus, similar to the alternative pathways, well below that of fossil diesel ($86 \text{ g}_{\text{CO}_2\text{-eq.}} \text{ MJ}^{-1}$) (Fig. S10, ESI†).

In total, methanol transfer-hydrogenation toward DMM can represent a promising pathway alternative if two prerequisites can be satisfied: significant catalyst improvements allowing a higher single-pass DMM yield and a more promising H₂ carrier substance. Such a substance can be more promising either in terms of a higher efficiency regarding H₂ management, or in terms of value as a final by-product.

A summary of the existing bottlenecks connected to each reaction pathway is given in ESI,† Table S18. To support future research in DMM synthesis, we therein estimate the significance of each bottleneck's impact on KPIs and propose improvement measures correspondingly.

5 Conclusions

Extensive effort in catalyst development for dimethoxymethane (DMM) production during the last years have resulted in remarkably improved reaction performances and completely new reaction pathways. Yet, the achievements in catalyst development have not been assessed from a process perspective such that their actual performance and sustainability for industrial applications still remain unknown. In this paper, we demonstrate that DMM produced *via* different reaction pathways offers considerable benefits compared to fossil diesel if requirements on cost and carbon footprint of raw material provision are met. However, for each individual pathway special aspects for their further development need to be addressed if those requirements can not be fulfilled to an arbitrary large extent.

Our hierarchical process evaluation shows that comparable process efficiencies to other e-fuels (*e.g.*, dimethyl ether (DME)) can only be achieved if H₂ consumption is low. The non-oxidative pathways (reductive, dehydrogenative, and transfer-hydrogenative pathway) have a maximum exergy efficiency of 97% (Level 1), which is significantly higher than that of the established and oxidative pathway and most other e-fuels. More detailed process analyses (Level 2 and 3) of all pathways reveal that exergy losses mainly result from an energy-intensive product separation and a low DMM single-pass yield of current catalysts. Although these losses are more pronounced for the non-oxidative reaction pathways, their exergy efficiency is higher than that of the established and oxidative one. Their comparably low H₂ consumption is key for efficient DMM production-especially in a world with limited renewable electricity.

The production cost for DMM may fall below the price of fossil diesel only if H₂ can be produced for less than $4\$ \text{ kg}^{-1}$



and if a low H_2 consumption can be ensured. Cost competitiveness with fossil diesel is most likely achievable for the reductive pathway already for the current catalyst performance. It is also the only pathway that is currently cost-competitive with the production of other e-fuels.

In terms of the impact on climate change of DMM, the pathways do not differ significantly from one another if exclusively renewable electricity is utilized. In this case, DMM has the potential to reduce its climate impact by up to 92% compared to fossil diesel. In contrast, if the impact on climate change of electricity supply increases to that of Finland or Switzerland (up to $190 \text{ gCO}_2\text{-eq. kW h}^{-1}$), it does matter which pathway is used for DMM production from a climate impact perspective. In this range, the currently high heat demand and co-production of side products make the impact on climate change of the dehydrogenative pathway being most dependent on the impact on climate change of electricity supply. The climate impact of the reductive pathway is least dependent on the electricity carbon-intensity and is lower than that of fossil diesel below $190 \text{ gCO}_2\text{-eq. kW h}^{-1}$. For an even higher carbon-intensity of electricity supply, DMM should not be considered as an alternative fuel since its impacts on climate change would exceed those of fossil diesel.

In contrast to the established and oxidative pathway, the non-oxidative pathways have been proposed just recently such that their catalyst performances are expected to still improve significantly. For exploiting the full potential of these pathways and ultimately deciding which one is suited most for sustainable DMM production, more research need to be conducted. For the dehydrogenative pathway, future catalyst development need to aim at suppressing side reactions even more effectively. Alternatively, a systematic exploitation of the co-products in a multi-product plant for producing different e-fuels (e.g., DMM, DME, and methyl formate) should be evaluated. For the transfer-hydrogenative pathway, future experimental studies should aim not exclusively at increasing turnover numbers, but also increasing single-pass DMM yield. Together with the identification of an industrially viable hydrogen carrier substance, comparable performance indicators to those of the reductive pathway can be achieved. The reductive pathway is the most developed one among the non-oxidative pathways. We have shown that already with a catalyst at its current state, an efficient DMM production at competitive cost and low climate impact is possible in some countries. To reach the next stage of development, the handling of the homogeneous catalyst needs to be analyzed.

Author contributions

J. Burre developed the concept of the study and proposed the process development and evaluation methodology. J. Burre and D. Bongartz developed the processes and performed process optimization under the supervision of A. Mitsos. J. Burre and D. Bongartz evaluated the processes regarding efficiency. J. Burre calculated production costs. S. Deutz and S. Völker calculated the impact on climate change supervised by A. Bardow and wrote corresponding sections of the manuscript.

C. Mebrahtu, O. Osterthun, and R. Sun wrote the descriptions of the novel reaction pathways and provided fundamental information for the discussions regarding catalyst improvement potential under the supervision of J. Klankermayer and R. Palkovits. J. Burre wrote the rest of the manuscript. All authors contributed to the discussions and revisions of the manuscript.

Conflicts of interest

There are no conflicts to declare.

Acknowledgements

The authors gratefully acknowledge funding by the German Federal Ministry of Education and Research (BMBF) within the Kopernikus Project P2X: Flexible use of renewable resources – exploration, validation and implementation of “Power-to-X” concepts (FKZ 03SF0566P0) and the project NAMOSYN: Nachhaltige Mobilität durch synthetische Kraftstoffe (FKZ 03SF0566P0). This work is further funded by Deutsche Forschungsgesellschaft (DFG, German Research Foundation) under Germany's Excellence Strategy – Cluster of Excellence 2186 “The Fuel Science Center” – ID: 390919832.

References

- 1 BP, *BP Energy Outlook: 2019 edition*, 2019, <https://www.bp.com/content/dam/bp/business-sites/en/global/corporate/pdfs/energy-economics/energy-outlook/bp-energy-outlook-2019.pdf>, Accessed: 2020-01-21.
- 2 M. Contestabile, G. J. Offer, R. Slade, F. Jaeger and M. Thoenes, *Energy Environ. Sci.*, 2011, **4**, 3754–3772.
- 3 E. Çabukoglu, G. Georges, L. Küng, G. Pareschi and K. Boulouchos, *Transp. Res. Part C: Emerging Technol.*, 2018, **88**, 107–123.
- 4 D. Pélerin, K. Gaukel, M. Härtl, E. Jacob and G. Wachtmeister, *Fuel*, 2020, **259**, 116231.
- 5 M. Härtl, K. Gaukel, D. Pélerin and G. Wachtmeister, *MTZ - Motortech. Z.*, 2017, **78**, 52–59.
- 6 A. García, J. Monsalve-Serrano, D. Villalta, R. L. Sari, V. G. Zavaleta and P. Gaillard, *Appl. Energy*, 2019, **253**, 113622.
- 7 M. Härtl, P. Seidenspinner, E. Jacob and G. Wachtmeister, *Fuel*, 2015, **153**, 328–335.
- 8 A. Omari, B. Heuser and S. Pischinger, *Fuel*, 2017, **209**, 232–237.
- 9 S. E. Iannuzzi, C. Barro, K. Boulouchos and J. Burger, *Fuel*, 2017, **203**, 57–67.
- 10 A. Omari, B. Heuser, S. Pischinger and C. Rüdinger, *Appl. Energy*, 2019, **239**, 1242–1249.
- 11 IEA, International Energy Agency, *Energy Efficiency Indicators - Highlights*, 2020.
- 12 L. Ding, T. Shi, J. Gu, Y. Cui, Z. Zhang, C. Yang, T. Chen, M. Lin, P. Wang, N. Xue, L. Peng, X. Guo, Y. Zhu, Z. Chen and W. Ding, *Chem*, 2020, **6**, 2673–2689.



- 13 N. Mahbub, A. O. Oyedun, A. Kumar, D. Oestreich, U. Arnold and J. Sauer, *J. Cleaner Prod.*, 2017, **165**, 1249–1262.
- 14 A. O. Oyedun, A. Kumar, D. Oestreich, U. Arnold and J. Sauer, *Biofuels, Bioprod. Biorefin.*, 2018, **12**, 694–710.
- 15 X. Zhang, A. O. Oyedun, A. Kumar, D. Oestreich, U. Arnold and J. Sauer, *Biomass Bioenergy*, 2016, **90**, 7–14.
- 16 S. Schemme, R. C. Samsun, R. Peters and D. Stolten, *Fuel*, 2017, **205**, 198–221.
- 17 D. Bongartz, J. Burre and A. Mitsos, *Ind. Eng. Chem. Res.*, 2019, **58**, 4881–4889.
- 18 J. Burre, D. Bongartz and A. Mitsos, *Ind. Eng. Chem. Res.*, 2019, **58**, 5567–5578.
- 19 M. Held, Y. Tönges, D. Pélerin, M. Härtl, G. Wachtmeister and J. Burger, *Energy Environ. Sci.*, 2019, **12**, 1019–1034.
- 20 S. Deutz, D. Bongartz, B. Heuser, A. Käthelhorn, L. S. Langenhorst, A. Omari, M. Walters, J. Klankermayer, W. Leitner, A. Mitsos, S. Pischinger and A. Bardow, *Energy Environ. Sci.*, 2018, **11**, 331–343.
- 21 L. Lautenschütz, D. Oestreich, P. Seidenspinner, U. Arnold, E. Dinjus and J. Sauer, *Fuel*, 2016, **173**, 129–137.
- 22 D. Bongartz, L. Doré, K. Eichler, T. Grube, B. Heuser, L. E. Hombach, M. Robinius, S. Pischinger, D. Stolten, G. Walther and A. Mitsos, *Appl. Energy*, 2018, **231**, 757–767.
- 23 Z. P. Cano, D. Banham, S. Ye, A. Hintennach, J. Lu, M. Fowler and Z. Chen, *Nat. Energy*, 2018, **3**, 279–289.
- 24 K. D. Vertin, J. M. Ohi, D. W. Naegeli, K. H. Childress, G. P. Hagen, C. I. McCarthy, A. S. Cheng and R. W. Dibble, *Methylal and Methylal-Diesel Blended Fuels for Use in Compression-Ignition Engines*, SAE Technical Paper Series, 1999.
- 25 J. Schröder and K. Görsch, *Energy Fuels*, 2020, **34**, 450–459.
- 26 G. Reuss, W. Disteldorf, A. Gamer and A. Hilt, *Formaldehyde*, Ullmann's Encyclopedia of Industrial Chemistry, 2000.
- 27 J. Burger, E. Ströfer and H. Hasse, *Chem. Eng. Res. Des.*, 2013, **91**, 2648–2662.
- 28 N. Schmitz, J. Burger, E. Ströfer and H. Hasse, *Fuel*, 2016, **185**, 67–72.
- 29 A. Peter, S. M. Fehr, V. Dybbert, D. Himmel, I. Lindner, E. Jacob, M. Ouda, A. Schaadt, R. J. White, H. Scherer and I. Krossing, *Angew. Chem.*, 2018, **130**, 9605–9608.
- 30 A. Peter, G. Stebens, J. F. Baumgärtner, E. Jacob, F. K. Mantei, M. Ouda and I. Krossing, *ChemCatChem*, 2020, **12**, 2416–2420.
- 31 J. Walker, *Formaldehyde*, Reinhold Publishing, 1944.
- 32 C. Kuhnert, M. Albert, S. Breyer, I. Hahnenstein, H. Hasse and G. Maurer, *Ind. Eng. Chem. Res.*, 2006, **45**, 5155–5164.
- 33 H. Liu, H. Gao, Y. Ma, Z. Gao and W. Eli, *Chem. Eng. Technol.*, 2012, **35**, 841–846.
- 34 Q. Wang, B. Yu and C. Xu, *Ind. Eng. Chem. Res.*, 2012, **51**, 1281–1292.
- 35 B. Yu, Q. Wang and C. Xu, *Ind. Eng. Chem. Res.*, 2012, **51**, 1293–1310.
- 36 X. Zhang, S. Zhang and C. Jian, *Chem. Eng. Res. Des.*, 2011, **89**, 573–580.
- 37 J.-O. Weidert, J. Burger, M. Renner, S. Blagov and H. Hasse, *Ind. Eng. Chem. Res.*, 2017, **56**, 575–582.
- 38 R. Sun, I. Delidovich and R. Palkovits, *ACS Catal.*, 2019, **9**, 1298–1318.
- 39 K. Thenert, K. Beydoun, J. Wiesenthal, W. Leitner and J. Klankermayer, *Angew. Chem.*, 2016, **128**, 12454–12457.
- 40 K. Roh, A. Bardow, D. Bongartz, J. Burre, W. Chung, S. Deutz, D. Han, M. Heßelmann, Y. Kohlhaas, A. König, J. S. Lee, R. Meys, S. Völker, M. Wessling, J. H. Lee and A. Mitsos, *Green Chem.*, 2020, **22**, 3842–3859.
- 41 A. W. Zimmermann and R. Schomäcker, *Energy Technol.*, 2017, **5**, 850–860.
- 42 J. A. Bergerson, A. Brandt, J. Cresko, M. Carbajales-Dale, H. L. MacLean, H. S. Matthews, S. McCoy, M. McManus, S. A. Miller, W. R. Morrow, I. D. Posen, T. Seager, T. Skone and S. Sleep, *J. Ind. Ecol.*, 2019, **24**, 11–25.
- 43 G. Thomassen, M. V. Dael, S. V. Passel and F. You, *Green Chem.*, 2019, **21**, 4868–4886.
- 44 S. Su, P. Zaza and A. Renken, *Chem. Eng. Technol.*, 1994, **17**, 34–40.
- 45 B. G. Schieweck and J. Klankermayer, *Angew. Chem.*, 2017, **129**, 10994–10997.
- 46 M. Siebert, M. Seibicke, A. F. Siegle, S. Kräh and O. Trapp, *J. Am. Chem. Soc.*, 2019, **141**, 334–341.
- 47 R. Sun, C. Mebrahtu, J. P. Hofmann, D. Bongartz, J. Burre, C. H. Gierlich, P. J. Hausoul, A. Mitsos and R. Palkovits, *Sustainable Energy Fuels*, 2021, **5**(1), 117–126.
- 48 O. Osterthun and J. Klankermayer, *Angew. Chem.*, submitted.
- 49 K. Kraemer, S. Kossack and W. Marquardt, *Ind. Eng. Chem. Res.*, 2009, **48**, 6749–6764.
- 50 J. Bausa, R. v. Watzdorf and W. Marquardt, *AIChE J.*, 1998, **44**, 2181–2198.
- 51 Process Systems Engineering (AVT.SVT), *EE-Toolbox*, 2017, <https://www.avt.rwth-aachen.de/cms/AVT/Forschung/Software/iptv/Shortcut-Toolbox/?lidix=1>, Accessed: 2020-03-04.
- 52 S. Kossack, K. Kraemer and W. Marquardt, *Ind. Eng. Chem. Res.*, 2006, **45**, 8492–8502.
- 53 J. Burre, D. Bongartz, L. Brée, K. Roh and A. Mitsos, *Chem. Ing. Tech.*, 2019, **92**, 74–84.
- 54 International Organization for Standardization, *ISO 14040: Environmental Management: Life Cycle Assessment: Principles and Framework*, ISO, 2006.
- 55 International Organization for Standardization, *ISO 14044: Environmental Management: Life Cycle Assessment: Requirements and Guidelines*, ISO, 2006.
- 56 L. J. Müller, A. Käthelhorn, M. Bachmann, A. Zimmermann, A. Sternberg and A. Bardow, *Front. Energy Res.*, 2020, **8**, 15.
- 57 J. Guinée, *Int. J. Life Cycle Assess.*, 2001, **6**, 255.
- 58 É. S. Van-Dal and C. Bouallou, *J. Cleaner Prod.*, 2013, **57**, 38–45.
- 59 J.-O. Drunsel, M. Renner and H. Hasse, *Chem. Eng. Res. Des.*, 2012, **90**, 696–703.
- 60 D. Bongartz, J. Burre, A. Ziegler and A. Mitsos, in *Computer Aided Chemical Engineering: 31st European Symposium on Computer Aided Process Engineering (ESCAPE 31)*, ed. M. Türkay and R. Gani, Power-to-OME₁ via Direct Oxidation



- of Methanol: Process Design and Global Flowsheet Optimization, 2021, in press.
- 61 T. Grube, L. Doré, A. Hoffrichter, L. E. Hombach, S. Rath, M. Robinius, M. Nobis, S. Schiebahn, V. Tietze, A. Schnettler, G. Walther and D. Stolten, *Sustainable Energy Fuels*, 2018, **2**, 1500–1515.
 - 62 M. Bui, C. S. Adjiman, A. Bardow, E. J. Anthony, A. Boston, S. Brown, P. S. Fennell, S. Fuss, A. Galindo, L. A. Hackett, J. P. Hallett, H. J. Herzog, G. Jackson, J. Kemper, S. Krevor, G. C. Maitland, M. Matuszewski, I. S. Metcalfe, C. Petit, G. Puxty, J. Reimer, D. M. Reiner, E. S. Rubin, S. A. Scott, N. Shah, B. Smit, J. P. M. Trusler, P. Webley, J. Wilcox and N. M. Dowell, *Energy Environ. Sci.*, 2018, **11**, 1062–1176.
 - 63 W. L. Luyben, *AIChE J.*, 2010, **57**, 655–670.
 - 64 W. D. Seider, J. D. Seader and D. R. Lewin, *Product & Process Design Principles: Synthesis, Analysis and Evaluation*, John Wiley & Sons, 2009.
 - 65 K. M. Guthrie, *Chem. Eng.*, 1969, **24**, 114–142.
 - 66 R. Turton, R. C. Bailie, W. B. Whiting and J. A. Shaeiwitz, *Analysis, synthesis and design of chemical processes*, Pearson Education, 2008.
 - 67 H. Li, Z. Song, X. Zhang, Y. Huang, S. Li, Y. Mao, H. J. Ploehn, Y. Bao and M. Yu, *Science*, 2013, **342**, 95–98.
 - 68 A. Linzenich, K. Arning, D. Bongartz, A. Mitsos and M. Ziefle, *Appl. Energy*, 2019, **249**, 222–236.
 - 69 R. Socolow, M. Desmond, R. Aines, J. Blackstock, O. Bolland, T. Kaarsberg, N. Lewis, M. Mazzotti, A. Pfeffer, K. Sawyer *et al.* Direct air capture of CO₂ with chemicals: a technology assessment for the APS Panel on Public Affairs, American physical society technical report, 2011.
 - 70 ecoinvent, *ecoinvent Database Version 3.01*, <https://ecoinvent.org/Search/Index>, Accessed: 2020-07-09.
 - 71 IEA, International Energy Agency, *Energy Technology Perspectives 2017: Catalysing Energy Technology Transformation*, 2017.
 - 72 A. Mitsos, I. Palou-Rivera and P. I. Barton, *Ind. Eng. Chem. Res.*, 2004, **43**, 74–84.

